1 **J. Bacteriol.**

2

3

4 # L-ascorbic acid (vitamin C) fermentation by the human

5 # pathogen *Vibrio cholerae*

6

7 **Rosenberger, J.R., N.D. McDonald, and E.F. Boyd**

8

9 **Department of Biological Sciences, University of Delaware, Newark, DE, 19716**

10 Corresponding author*

11 E. Fidelma Boyd

12 Department of Biological Sciences

13 341 Wolf Hall, University of Delaware

14 Newark, DE 19716

15 Phone: (302) 831-1088. Fax: (302) 831-2281 Email: fboyd@udel.edu

16

Abstract

17

18   L-ascorbic acid, commonly known as vitamin C, is a ubiquitous 6-carbon

19   carbohydrate characterized by its ability to scavenge free radicals. In enteric bacteria, L-

20   ascorbate can be utilized as a nutrient using the UlaABCDEF and UlaG-UlaRpathway

21   under anaerobic conditions. In this study, we identified homologs of the Ula system

22   within *Vibrio cholerae* and showed that *V. cholerae* is able to utilize L-ascorbate as an

23   energy source. Growth pattern assays of a *ulaG* in-frame deletion mutant demonstrated

24   that *ulaG* is essential for L-ascorbate fermentation. Expression analysis showed that *ula*

25   catabolism and transport genes were significantly induced in cells grown in the

26   presence of L-ascorbate compared to glucose and these genes were also highly induced

27   during growth on intestinal mucus. In *in vitro* growth competition assays, the *ulaG*

28   mutant was outcompeted by wild type when grown in intestinal mucus suggesting the

29   Ula system could be important for fitness. Within the *ula* operon in *V. cholerae* and all

30   *Vibrio* species a homology of ORF VCA0243 is present that encodes a pyridoxal

31   phosphate (PLP) phosphatase. This enzyme in *E. coli,* converts the active form of

32   vitamin B_6 PLP to its inactive form pyridoxal (PL). In *V. splendidus* and related species,

33   the aerobic and anaerobic L-ascorbate pathway genes cluster together and both systems

34   contain a PLP phosphatase. An in-frame deletion mutant of *vca0243* resulted in a

35   growth defect in L-ascorbate fermentation as well as additional carbon and amino acid

36   sources indicating a role in cellular metabolism. Phylogenetic analysis of UlaG and

37   UlaD suggested the region was acquired by horizontal gene transfer.

38

39   **Importance**

40   L-ascorbate is a carbohydrate present in the human intestine, available for microbial

41   consumption and several enteric species have been shown to utilize this compound as

42   an energy source. We demonstrated that L-ascorbate fermentation genes are also

43   present among marine bacteria from the family *Vibrionaceae* and that the human

44   pathogen *V. cholerae* can ferment L-ascorbate as an energy source. Within the Ula

45   operon in all *Vibrionaceae*, a putative pyridoxal phosphate phosphatase was present that

46   was required for L-ascorbate fermentation and cellular metabolism in general. The Ula

47   system was present among a limited number of genera within *Vibrionaceae; Vibrio,*

48   *Aliivibrio* and *Photobacterium* and showed an evolutionary history consistent with

49   horizontal transfer between genera and species.

50

51

52

53

Introduction

L-Ascorbic acid is a ubiquitous six-carbon carbohydrate known for its role as an antioxidant. It is also an essential nutrient, found within GI tissues, gastric juices as well as the mucosa, required for enzyme function and tissue repair in humans and other animals (1-3). Some higher order eukaryotes, such as humans, have lost the ability to biosynthesize ascorbate (4-6). In these species, the requirement for ascorbate is met through dietary intake(4, 5).

It is known that enteric bacteria are capable of utilizing L-ascorbate as a carbon and energy source (7-12). In *E. coli*, two systems exist for the catabolism of L-ascorbate, the Ula system and the YiaK-YiaS system. The Ula system is required for the fermentation of L-ascorbate under anaerobic conditions, whereas under aerobic conditions, both the Ula system and the YiaK-YiaS system are required. Studies in *E. coli* and *Klebsiella pneumoniae* show neither can aerobically catabolize L-ascorbate as a sole carbon source due to the reactivity of this molecule, and the generation of oxidative stress (7-12). Thus, aerobic catabolism of L-ascorbate requires the presence of specific amino acids (proline, threonine, or glutamine) in the culture medium that are proposed to decrease L-ascorbate oxidation (9, 10).

The gene cluster in *E. coli* responsible for L-ascorbate fermentation consists of the *ulaABCDEF* operon, and divergently transcribed genes *ulaG* and *ulaR* (7, 11, 13) (**Fig.**

73 **1A**). The *ulaABC* genes encode a phosphotransferase system (PTS) transporter for L-

74 ascorbate uptake during both anaerobic and aerobic growth (9, 10, 12). The *ulaDEF* and

75 *ulaG* genes are required for catabolism and *ulaR* encodes a regulator that acts as a

76 repressor (7, 11, 13). L-ascorbate is converted to D-xylulose-5P, which can be further

77 catabolized via the pentose phosphate pathway (7, 11, 13) (**Fig. 1B**). Regulation of the

78 Ula system in *E. coli* is under the control of UlaR, cAMP-receptor protein (CRP), as well

79 as integration host factor (IHF) (9, 10). Both IHF and UlaR act as repressors, while CRP

80 is an activator of the *ulaABCDEF* operon (13). The Yia system shares three paralogous

81 proteins with the Ula system, UlaD/YiaQ, UlaE/YiaR and UlaF/YiaS, which share less

82 than 60% protein homology (**Fig. 1B**).

83   *Vibrio cholerae* is a ubiquitous marine bacterium that is also an enteric pathogen of

84 humans, and the causative agent of the deadly diarrheal disease, cholera. *V. cholerae* can

85 colonize the small intestine of humans, where it produces cholera toxin that causes the

86 secretory rice watery diarrhea, characteristic of cholera (14-17). Within the small

87 intestine *V. cholerae* competes with the indigenous microbiota for nutrients and has to

88 overcome many antagonistic interactions with the host microbiome (18-22). The

89 nutrients *V. cholerae* utilize *in vivo* are poorly understood, but it was shown that this

90 bacterium utilizes sialic acid, a component of intestinal mucus, as a sole carbon source

91 and this ability has a significant fitness advantage *in vivo* (23-25). Additionally, *V.*

92   *cholerae* was shown to use citrate fermentation *in vivo*, proposed to be an important

93   phenotype for long-term carriage of *V. cholerae* (18).

94   In this study, we identified L-ascorbate fermentation *ula* gene clusters amongst

95   *Vibrio* species, and demonstrated that *V. cholerae* can ferment L-ascorbate as a carbon

96   and energy source. An in-frame deletion of *ulaG* (locus tag VCA0248) in *V. cholerae* was

97   examined for growth on L-ascorbate. The expression pattern of *ula* genes in cells grown

98   in the presence of L-ascorbate or intestinal mucus was determined. Additionally, we

99   investigated whether L-ascorbate utilization resulted in a competitive advantage for

100   cells grown in intestinal mucus. In *Aliivibrio fischeri, Vibrio* and *Photobacterium* species,

101   within the *ula* operon, a gene (*vca0243*) that encodes a pyridoxal phosphate phosphatase

102   homologous to YbhA from *Escherichia coli* is present. YbhA is an enzyme that converts

103   pyridoxal phosphate (active vitamin C) to pyridoxal (inactive vitamin C). An in-frame

104   deletion of *vca0243* in *V. cholerae* was examined to determine its effect on L-ascorbate

105   catabolism and cellular metabolism in general. The role of CRP in L-ascorbate

106   utilization was also investigated. Phylogenetic and genomic comparative analyses of

107   UlaG, UlaD and the Ula cluster suggested that the region was acquired multiple times

108   among *Vibrionaceae* and has a polyphyletic history.

109

110   **Results**

111 **Ascorbate metabolism genes present in *Vibrio* species**. The YiaQ protein from the

112 YiaKLMNOPQRS cluster and UlaG from the Ula cluster of *E. coli* K-12 were used as

113 seeds for BLASTp and psiBLAST analysis to identify L-ascorbate catabolism gene

114 clusters in *V. cholerae* N16961. No proteins were identified with similarity to YiaQ or any

115 other Yia protein within the *V. cholerae* N16961 genome. However, within chromosome

116 II of *V. cholerae* N16961, we identified a homolog of UlaG (VCA0248), which is an L-

117 ascorbic acid lactonase responsible for the first step in the catabolic pathway of L-

118 ascorbate. Adjacent to *ulaG* was a *ulaR* homolog, which encoded a transcriptional

119 repressor (7, 11, 13) (**Fig. 1A**). In *V. cholerae*, transcribed divergently from *ulaR-ulaG* was

120 a set of seven ORFs, VCA0240-VCA0246, in a predicted operon, which shared

121 homology with *ulaABCDEF* from *E. coli* (**Fig. 1A**). The first ORF VCA0246, was

122 annotated as UlaA and was a fusion of the *ulaA* and *ulaB* genes from *E. coli*, which

123 encoded components IIC and IIB of a phosphotransferase (PTS) system (**Fig. 1A**).

124 VCA0245 shared homology with UlaC, the IIA component of the PTS system. VCA0242

125 and VCA0241 encoded homologs of UlaD and UlaE, respectively. In *E. coli*, UlaD is a

126 putative decarboxylase that converts 3-keto-L-gulonate-6-P to L-xylulose-5P and UlaE is

127 an epimerase that converts L-xylulose-5P to L-ribulose-5P (**Fig. 1B**) (7, 11). VCA0244 is a

128 homolog of UlaF from *E. coli*, a 4-epimerase that converts L-ribulose-5P to D-xylulose-5-

129 P (**Fig. 1B**). In *V. cholerae*, the Ula system contains an additional ORF, VCA0243 that is

130 absent from the Ula system in enteric species. VCA0243 shares 40.44% percent identity,

131   with 98% query cover and an E-value of 6e-62 to YbhA, a pyridoxal phosphate

132   phosphatase in *E. coli*. A VCA0243 homolog was present within the Ula cluster in all

133   *Vibrio* species examined.

134   ***Vibrio cholerae* and *V. vulnificus* utilization of L-ascorbate**. Next, we determined

135   whether L-ascorbate can be used as an alternative carbon and energy source by *Vibrio*

136   species. To accomplish this, *V. cholerae* N16961, *V. vulnificus* CMCP6, *V. parahaemolyticus*

137   RIMD2210633 and *E. coli* BW25113 were grown in microaerophilic conditions for 48

138   hours in M9 minimal media supplemented with casamino acids (M9CAS), M9CAS

139   supplemented with 20mM glucose (M9CAS-Glucose), or M9CAS supplemented with

140   20mM L-ascorbate (M9CAS-Ascorbate). Casamino acids were added to growth media to

141   alleviate the effects of L-ascorbate oxidation, which results in the production of reactive

142   oxygen species (ROS) that are damaging to the cell (10). *Escherichia coli*, *V. cholerae* and

143   *V. vulnificus* all grew significantly better in M9CAS-Ascorbate than M9CAS, indicating

144   they can utilize L-ascorbate as an energy source (**Fig 2A-C**). As expected, *V.*

145   *parahaemolyticus*, showed no difference between growth in M9CAS and M9CAS-

146   Ascorbate as it does not contain the Ula gene cluster (**Fig. 2D**).

147   **The *ulaG* gene is essential for L-ascorbate fermentation**. We constructed an in-frame

148   deletion of *ulaG* (VCA0247) in *V. cholerae* N16961 to investigate its requirement in L-

149   ascorbate fermentation. The *ulaG* gene encodes an L-ascorbic acid lactonase, which is

150   responsible for the first step in the L-ascorbate catabolic pathway. The wild type and

151 Δ*ulaG* grown in LB 1%NaCl aerobically showed a similar pattern, indicating that the

152 mutant had no overall growth defect (**Fig. S1**). Next, Δ*ulaG* and wild type were grown

153 anaerobically for 48 hours in M9CAS, M9CAS-Glucose or M9CAS-Ascorbate. No

154 growth defects were observed for Δ*ulaG* when grown in M9CAS or M9CAS-Glucose

155 showing a similar growth pattern on both media (**Fig. S1**). However, Δ*ulaG* had a

156 growth defect compared to wild type when grown in M9CAS-Ascorbate, with a

157 significantly lower OD. These data show that *ulaG* is required for L-ascorbate

158 fermentation in *V. cholerae* (**Fig. 3**).

159 **The *ula* genes are induced in the presence of L-ascorbate and when grown on**

160 **intestinal mucus**. Expression of *ulaA* (*VCA0246*), *ulaR (VCA0247)* and *ulaG (VCA0248)*

161 was analyzed in *V. cholerae* cells grown in M9CAS-Ascorbate, M9CAS-Glucose, M9CAS

162 and M9-Mucus. In M9CAS-Ascorbate versus M9CAS-Glucose expression of *ulaA* was

163 upregulated 788-fold, expression of *ulaR* was upregulated 568-fold, and *ulaG* was

164 upregulated 1100-fold (**Fig. 4A**). To determine whether this induction was specific to L-

165 ascorbate, and not due to catabolic repression by glucose, gene expression of cells

166 grown in M9CAS-Ascorbate was also compared to cells grown in M9CAS without any

167 additional carbohydrate supplementation. Under these conditions, the *ulaA, ulaR* and

168 *ulaG* genes were significantly upregulated in M9CAS-Ascorbate compared to cells

169 grown in M9CAS (**Fig. 4B**). Taken together, this data shows that the *ula* genes are highly

170 induced in the presence of L-ascorbate.

171   Previous studies have shown that *Vibrio* species can utilize intestinal mucus as a

172   carbon and energy source (25-28). Therefore, we examined the expression pattern of the

173   *ula* genes in *V. cholerae* cells growth in M9-Mucus. The expression of *ulaA, ulaR*, and

174   *ulaG* genes were significantly upregulated in cells grown in M9-mucus compared to

175   M9CAS-glucose (**Fig. 4C**). Specifically, *ulaA* is upregulated 66-fold, *ulaR* is upregulated

176   34-fold and *ulaG* is upregulated 99-fold (**Fig. 4C**).

177   Next, we determined whether L-ascorbate fermentation provides a competitive

178   advantage for *V. cholerae*. Fitness of the *ulaG* mutant relative to wild type was evaluated

179   in *in vitro* competition assays in M9CAS-Ascorbate and M9CAS-mucus. Competitive

180   indices (CI) for growth on M9CAS-Ascorbate was less than 0.1 indicating that the wild

181   type outcompeted the *ulaG* mutant. Similarly, the CI in M9CAS-mucus was 0.55

182   demonstrating that the *ulaG* mutant was outcompeted by wild type suggesting that L-

183   ascorbate fermentation may be an important *in vivo* phenotype (**Fig. 5**).

184   **VCA0243 a pyridoxal 5′ phosphate (PLP) phosphatase homolog**. In *V. cholerae*, *vca0243*

185   (AAF96154.1) encodes a 272 amino acid protein that shows 40.44% homology with 98%

186   query cover to YbhA (VWQ01556.1) from *E. coli*. We constructed an in-frame deletion of

187   *vca0243* in *V. cholerae* N16961 and examined growth in LB 1%NaCl. The mutant grew

188   similar to wild type demonstrating no overall growth defect (**Fig. S2**). Next, we

189   examined growth in M9CAS, M9CAS-Glucose and M9CAS-Ascorbate under anaerobic

190   conditions. In M9CAS and M9CAS-glucose, the wild type and the mutant strains grew

191   similar to one another (data not shown). In M9CAS-Ascorbate, the mutant had a growth

192   defect compared to wild type with a significantly lower final OD (**Fig. 6A**) and in M9-

193   Ascorbate, the mutant was unable to grow in the absence of CAS (**Fig. 6B**). These data

194   indicates that *vca0243* is required for efficient L-ascorbate fermentation.

195   Deletion of *ybhA* in *E. coli* disrupted PLP homeostasis, causing growth inhibition

196   and the presence of casamino acids was shown to alleviate this inhibition (29). Thus, we

197   examined whether deletion of *vca0243* resulted in a growth defect in the absence of

198   casamino acids when grown aerobically in glucose (**Fig. 6C and 6D**). In M9CAS-

199   Glucose both wild type and the mutant grew similar, but in M9-Glucose, the mutant

200   had a growth defect demonstrated by a longer lag phase and a reduced final OD (**Fig.**

201   **6D**). Overall, these data suggest that the VCA0243 is an required for optimal growth in

202   the absence of casamino acids.

203   Next, we determined whether *vca0243* was important for growth on other carbon

204   sources in general. To accomplish this, we used PM1 Biolog phenotype microarray

205   growth assays to examine the utilization of 95 different carbon and energy sources by *V.*

206   *cholerae* wild type and Δ*vca0243*. We found there were significant differences between

207   wild type and Δ*vca0243* in 26 different carbon sources, which included amino acids or

208   amino acid derivatives (**Fig. S3**). The area under the curve (AUC) of wild type growth

209   was significantly higher than that of Δ*vca0243* in six of these amino acids, but

210   significantly greater than wild type in L-threonine (**Fig. S3**). Differences in growth were

211   also observed in 19 other carbon sources, with the wild-type strain utilizing these

212   compounds significantly better than Δ*vca0243* (**Fig. S3**). Overall, the data indicate that

213   VCA0243 has an important role in cellular metabolism.

214   **CRP is required for L-ascorbate fermentation in *V. cholerae*.** It is known that cAMP-

215   receptor protein (CRP) is a global regulator of alternative carbon metabolism in a

216   variety of bacterial species (30-32). CRP was shown to be a regulator of the both the Yia

217   and Ula system in *E. coli* and *K. pneumoniae* (9, 13). We constructed an in-frame deletion

218   of *crp* (VC2614) and examined growth in M9CAS-Glucose. The *crp* mutant grew similar

219   to wild type indicting no overall growth defect (**Fig. 7A**). Next, we examined growth

220   inM9CAS-Ascorbate and show that Δ*crp* had a significant growth defect compared to

221   wild type indicating that the mutant is unable to utilize L-ascorbate for growth (**Fig.**

222   **7B**).

223   **Phylogenetic analysis of UlaG and UlaD among *Vibrionaceae*.** To decipher the

224   evolutionary history of ascorbate fermentation genes within the *Vibrionaceae*, we

225   constructed a phylogenetic tree based on the UlaG and UlaD proteins. In addition, we

226   constructed a tree based on the housekeeping protein RpoB from the same set of strains,

227   as an indicator of the ancestral relationships among these species (33) (**Fig. S4**). On the

228   UlaG tree, UlaG proteins that are present in members of the *Vibrionaceae* clustered

229   within three major groups, which we designated A, B, and C, and encompassed 39

230   *Vibrio* species, *Aliivibrio fischeri* and 7 *Photobacterium* species (**Fig. 8**). Cluster A consists

231   of UlaG from *V. cholerae* and its sister species, *V. mimicus and V. metoecus*. Also, within

232   cluster A is UlaG from four members of the Campbellii clade, *V. harveyi, V. campbellii V.*

233   *jasicida* and *V. owensii*, while UlaG is absent from all other members of this clade, which

234   includes *V. parahaemolyticus* and *V. alginolyticus*.

235   Branching within cluster A, but divergently from *V. cholerae, V. mimicus* and *V.*

236   *metoecus,* is UlaG from four *Providencia* species, members of the family *Morganellaceae*.

237   However, the bootstrap value is low so this is likely not the origin of Ula from

238   *Providencia,* but does suggest a close relationship with *Vibrio*. Of the four *Providencia*

239   species that carry Ula, only *P. rettgeri* contained a *ybhA* homology within the *ula* cluster

240   *ulaABybhAulaD*, and is present in all 30 *P. rettgeri* genomes in the database. In *P.*

241   *alcalifaciens, P. rustigianii,* and *P. heimbachae,* the *ula* cluster consists of *ulaABD* with no

242   *ybhA* homolog. In all four *Providencia* species the *ulaE* and *ulaF* homologs were present

243   elsewhere on the genome (**Fig. S4**). The phylogenetic tree based on a housekeeping

244   protein RpoB showed that the *Providencia* species clustered together divergent from

245   *Vibrio* species, and are not closely related to *Vibrio* (**Fig S4**).

246   Within cluster B are *Vibrio* species belonging to the Splendidus clade, which

247   cluster closely together; within this group is UlaG from *Aliivibrio fischeri* and

248   *Photobacterium damselae* strains (**Fig. 8**). The positioning of UlaG from these species,

249   nested within UlaG from *Vibrio* species, suggest the region has an origin in *Vibrio.* This

250   is further evidenced by the RpoB tree showing that species from these genera cluster

251   separately and distantly from *Vibrio* species (**Fig. S4**). Cluster C contained three groups

252   of *Vibrio* species interspersed with UlaG from five *Photobacterium* species. The bootstrap

253   values associated with *Photobacterium* species branching are extremely low indicating

254   that the precise relationship with Vibrio species cannot be determined but does indicate

255   a *Vibrio* origin for UlaG. Branching divergently from clusters A, B, and C is a single

256   UlaG from *V. tritonius*.

257   The nearest relative to UlaG from *Vibrio* outside of cluster A, B and C is UlaG

258   from *Yersinia ruckerii* and *Y. nurmii*, which branched together but divergently from

259   *Vibrio* species. The next most closely related UlaG protein is from *Gilliamella apicola* and

260   *G. apis*, gut symbionts of honeybees. *Gilliamella* is member of the *Orbaceae* family, a sister

261   taxon to the order *Enterobacteriales* (34). In these species, the *ula* cluster is similar to

262   *Vibrio* in terms of gene order but does not contain a *ybhA* homolog. The last group of

263   UlaG proteins to cluster with UlaG from *Vibrio*, are UlaG from *Dickeya zeae*, *Yersinia*

264   *intermedia* and five *Aeromonas* species. The *ula* genes are present in two divergently

265   transcribed operons *ulaABFD* and *ulaGybhAER* in *Y. intermedia* and *Aeromonas* species,

266   whereas in *D. zeae*, the *ula* genes are arranged *ulaABD* and *ulaGER* (**Fig. S4**). These are

267   the only *Yersinia* and *Aeromonas* species, of the 12 described within *Yersinia* and the 14

268   within *Aeromonas* that contain the ascorbate fermentation gene cluster.

269   Given that *ulaG* and *ulaR* are divergently transcribed from the Ula transport and

270   catabolism operon, we constructed a phylogenetic tree based on UlaD to determine

271   whether the operon has a similar evolutionary history to UlaG. The UlaD tree showed

272   some congruence among the genera in terms of their location within the tree (**Fig. S5**).

273   However, the UlaD protein among *Vibrio* species showed low bootstrap values making

274   comparisons among *Vibrio* species unreliable. UlaD from five *Photobacterium* species

275   branched with the *Vibrio* UlaD proteins, but clustered at different locations with low

276   bootstrap values. In addition, two *Photobacterium* species branched with UlaD from

277   *Yersinia* and *Gilliamella* species but again the bootstrap value was very low indicating

278   the exact placement of UlaD within the tree is hard to define. However, the placement

279   of UlaD and UlaG proteins from *Photobacterium* species at different locations within the

280   trees is in direct contrast to their branching together within the RpoB tree. *Aliivibrio*

281   *fischeri* UlaD clustered with UlaD from the Splendidus clade, similar to UlaG and again

282   this is in contrastto RpoB a locus ancestral to the species (**Fig. S4 and S5**). UlaD from *V.*

283   *scophthalmi* was the most divergent protein examined in *Vibrio* and branched distantly

284   from all other species. The UlaG protein from this species also branched divergently.

285   Examination of the genome context of the Ula region in *V. scophthalmi* showed that the

286   region was present on a plasmid pVS53 and thus was likely acquired by horizontal gene

287   transfer.

288   Interestingly, analysis of L-ascorbate catabolism genes among members of the

289   Splendidus clade identified a second YbhA homolog in these species (**Fig. S6**). This

290   *ybhA* gene clustered with *yia* genes required for aerobic respiration of L-ascorbate and

291   these genes were contiguous with the *ula* gene cluster (**Fig. S6**). This is a unique

292   grouping of the aerobic and anaerobic L-ascorbate catabolism genes in these species and

293   the presence of a YbhA homolog within each cluster suggests a critical role for YbhA in

294   the L-ascorbate catabolism pathways.

Discussion

296   In this study, we identified homologs of the Ula L-ascorbate fermentation cluster

297   in *V. cholerae* and other *Vibrio* species. Growth pattern analysis revealed that *V. cholerae*

298   and *V. vulnificus* could utilize L-ascorbate as an alternative nutrient source. In *V.*

299   *cholerae*, we demonstrated that the *ulaG* gene is required for L-ascorbate fermentation

300   and that the *ula* genes are induced in the presence of L-ascorbate. Our *in vitro*

301   competition assays showed that Δ*ulaG* was outcompeted by wild type in M9CAS-

302   Mucus indicting that L-ascorbate catabolism provides a fitness advantage. We also

303   demonstrated that deletion of *crp* in *V. cholerae* resulted in a defect in growth, indicating

304   that L-ascorbate fermentation is also under the control of CRP in this species.

305   Overall, out data suggest that L-ascorbate utilization is likely an important

306   phenotype that may provide a fitness advantage *in vivo*. Previous studies in two human

307   pathogens have suggested that ascorbate catabolism may be important for host

308   colonization. Recent proteomics analysis of enterohemorrhagic *E. coli* (EHEC) in

309   gnotobiotic piglets showed that some of the most differentially abundant proteins

310   during infection were involved in L-ascorbate metabolism (35). Additionally, dual

311   RNA-seq, RT-qPCR and metabolomics analysis of *H. ducreyi* in a human infection

312   model demonstrated that genes associated with L-ascorbate recycling are upregulated

313   in human hosts, while the most upregulated genes in *H. ducreyi* are the *ula* genes

314   required for L-ascorbate fermentation (36).

315   We identified a homologue of a PLP phosphatase within the *ula* operon, encoded

316   by VCA0243, that we showed is essential for growth on L-ascorbate in the absence of

317   casamino acids, and also was required for efficient growth on several amino acids and

318   sugars. PLP is a cofactor for many proteins and enzymes involved in a variety of

319   cellular processes, including amino acid biosynthesis and degradation, as well as carbon

320   metabolism (29, 37-39). It is widely known that PLP-dependent enzymes are associated

321   with biochemical pathways that involve amino acids (39). A recent study in *E. coli*

322   demonstrated that excess accumulation of either PL and PLP results in inhibition of

323   growth initiation and changes in amino acid profiles (29). Growth initiation inhibition

324   caused by PL or PLP accumulation was alleviated by addition of exogenous casamino

325   acids to growth media (29). In *V. cholerae*, VCA0243 is likely a PLP phosphatase

326   responsible for the dephosphorylation and inactivation of PLP, which could explain the

327   growth defects of Δ*vca0243* in the absence of casamino acids. The remarkable clustering

328   of both aerobic and anaerobic L-ascorbate catabolism genes in V. splendidus and

329   related species and the presence of a YbhA homolog, which we named UlaP within

330   each cluster, suggests the importance of PLP phosphatase in these pathways.

331   Our phylogenetic analysis showed that L-ascorbate fermentation genes are

332   present in a subset of *Vibrio* species, a single *Aliivibrio* species, and seven *Photobacterium*

333   species. For *Aliivibrio fischeri* and *Photobacterium* species, the UlaG and UlaD proteins

334   clustered with *Vibrio* species suggests horizontal transfer among these groups.

335   Similarly, UlaG and UlaD proteins from *Providencia* species clustered with those from

336   *Vibrio* species but the gene order is very different, indicating that this relationship is

337   ancient. It is of interest to note that the *ula* genes from *A. fischeri* and *Providencia* species

338   are located close to the *glmS* locus, which is the site of insertion of the transposon Tn7 in

339   *E. coli*. In *Pr. heimbachae*, adjacent to the *ula* genes inserted at the *glmS* locus, is a Tn7

340   operon *tnsABCDE*. This may suggest a mode of acquisition of the *ula* genes in this

341   species. In *Ph. damselae* strains that contain the *ula* cluster, the region is flanked on one

342   side by a phage-like tyrosine recombinase integrase and the other end is flanked by

343   phage genes and a restriction modification system. These genes are also present in *Ph.*

344   *phosphoreum* strains that contain *ula* genes. In *Y. intermedia* directly adjacent to *ulaD* is a

345   CRISPR repeat region and a type I-F CRISPR-Cas gene cluster followed by an integrase.

346   In *A. veronii*, adjacent to *ulaD* is a tyrosine recombinase integrase. Finally, in *V.*

347   *scophthalmi*, the *ula* genes were present on a plasmid again suggesting a mode of

348   acquisition. Thus, along with our phylogenetic analysis, these signatures of horizontal

349   gene transfer strongly suggest a polyphyletic origin for Ula and multiple acquisition

350   events among species.

351   **Material and Methods**

352   **Bacterial strains.** *Vibrio cholerae* and *E. coli* were cultured aerobically with shaking

353   (225rpm) in Luria Bertaini (LB) broth (Fisher Scientific, Waltham, MA) containing 1%

354   NaCl at 37°C. *V. vulnificus* and *V. parahaemolyticus* were similarly cultured in LB

355   containing a final concentration of 2% and 3% NaCl, respectively. Where indicated, M9

356   minimal media was utilized and supplemented with 0.02 mM $MgSO_4$, and 0.1 mM

357    $CaCl_2$. Additionally, media was supplemented with 25 µg/mL of chloramphenicol (Cm)

358   when required during mutant construction.

359   **Growth pattern analysis.** *Vibrio cholerae* N16961 wild type and mutant strains were

360   grown overnight at 37°C in LB 1% NaCl (LB 1%) with aeration, pelleted by

361   centrifugation, washed with 1xPBS, and then resuspended in 1xPBS. Aerobic growth

362   assays conducted in M9 minimal media containing 1% NaCl (M9) supplemented with

363   20mM glucose (M9-Glucose) or M9 containing 2% (w/v) casamino acids (M9CAS) (MP

364   Biomedicals, LLC. Solon, OH) supplemented with 20mM glucose (M9CAS-Glucose) or

365   with 20mM L-ascorbate (M9CAS-Ascorbate). Cultures were incubated at 37°C for 24

366   hours with intermittent shaking. OD_{595nm} was measured every hour utilizing a Tecan

367   Sunrise (Tecan Group Ltd., Männedorf, Switzerland) microplate reader. A minimum of

368   2 biological replicates were performed for each condition. The mean OD_{595nm} and

369   standard deviation of biological replicates was calculated for each assay. To create a

370   microaerophilic environment, the cultures were aliquoted into fully filled snap-cap

371   tubes and incubated statically at 37°C. At each time point, a sample was taken,

372   centrifuged and resuspended in 1xPBS prior to measuring OD_{600nm}. The concentration of

373   NaCl was adjusted to 1% for *E. coli*, 2% for *V. cholerae* and *V. vulnificus*, and 3% for *V.*

374   *parahaemolyticus* in each respective media. All microaerophilic growth assays included a

375   minimum of three biological replicates. Anaerobic conditions were created by

376   incubating microplates in airtight containers containing GasPak EZ Anaerobe sachets

377   (BD Diagnostics, Sparks, MD). The OD_{595nm} of cultures was measured every 12 hours

378   using a Tecan Sunrise spectrophotometric microplate reader. All assays were performed

379   with a minimum of two biological replicates. The mean and standard deviation of

380   biological replicates were calculated for each growth condition. End-point biomass

381   comparisons were performed using an unpaired Students *t*-test with 95% confidence

382   interval.

383   **Real time quantitative PCR (qPCR).** RNA was extracted from wild-type *V. cholerae*

384   N16961 in M9 media supplemented with 0.02% (w/v) casamino acids (M9CAS),

385   M9CAS+20 mM glucose (M9CAS-Glucose), or M9CAS+20 mM L-ascorbic acid (M9CAS-

386   Ascorbate) and M9 supplemented with 20 mM glucose (M9-Glucose) or mouse

387 intestinal mucus (M9-Mucus). Following 90 minutes of static growth at 37°C, RNA was

388 isolated using TRIzol RNA extraction protocol according to the manufacturer's

389 instructions, and subsequently treated with Turbo DNase (Invitrogen). Purified RNA

390 was quantified via Nanodrop spectrophotometer (Thermo Scientific, Waltham, MA)

391 and 500 ng was used as a template for cDNA synthesis using Superscript III reverse

392 transcriptase (Invitrogen). A 1:25 dilution of each cDNA sample was used for

393 quantitative real-time PCR (qPCR). qPCR was carried out on a QuantStudio™ 6 Flex

394 System with cycling parameters of a hold stage of 95°C for 20 s followed by a cycling

395 stage of 95°C for 1 s and 60°C for 20 s. Relative gene expression was determined with

396 Quantstudio Real-Time PCR Software v1.2 following the comparative C_T ($\Delta\Delta C_T$)

397 method (40). The qPCR primers for *vca0246*, *vca0247*, and *vca0248* are listed in Table S1.

398 Gene expression was normalized to the housekeeping gene for topoisomerase I (*topI*)

399 listed in Table S1. RNA was isolated from two independent biological replicates and

400 qPCR was performed in duplicate. Statistical analysis was performed comparing mean

401 ΔC_T for a given target gene using a Student's t-test with a 95% confidence interval

402 **In-frame deletion of *vca0243*, *ulaG* and *crp* (VC2614) construction.** An in-frame

403 *vca0243* deletion mutant was constructed via splicing by overlap-extension (SOE) and

404 homologous recombination (41). The genome sequence of *V. cholerae* N16961 was used

405 to design primers to create a 225-bp truncated *vca0243* PCR product. Gene fragments

406 were amplified using primer pairs VCA0243_A/VCA0243_B and

407   VCA0243_C/VCA0243_D, then digested via SacI and XbaI. The digested fragments were

408   ligated with SacI and XbaI linearized pDS132, then transformed into *E. coli* DH5αλ*pir*.

409   Plasmid DNA was isolated from DH5α using the Nucleospin Plasmid kit

410   (MACHEREY-NAGEL Inc., Bethlehem, PA) and transformed into the DAP-auxotroph

411   donor strain *E. coli* β2155λ*pir*. The donor strain was conjugated overnight with the

412   recipient strain *V. cholerae* N16961 on LB 1% plates. Selection of *V. cholerae* strains that

413   had integrated deletion vectors into the genome was performed by plating conjugations

414   on LB 1% plates containing Cm and confirmed by PCR. Colonies were then grown

415   overnight without selection in LB 1% and plated on LB 1% supplemented with 10%

416   sucrose (w/v) to select for strains that had undergone a second homologous

417   recombination event. The genome sequence of *V. cholerae* N16961 was utilized to design

418   primers for generation of a 110-bp truncated *ulaG* PCR product, and a 30-bp truncated

419   *crp* PCR product. In-frame deletions of *ulaG* (*VCA0248*) and *crp* (*VC2614*) were

420   constructed using a Gibson assembly protocol and HiFi DNA assembly master mix

421   (New England Biolabs, Ipswich, MA). Gene fragments were amplified using primer

422   pairs VC_ulaG_A/VC_ulaG_B and VC_ulaG_C/VC_ulaG_D or VC_CRP_A/VC_CRP_B

423   and VC_CRP_C/VC_CRP_D. The resulting products were ligated and cloned into SacI

424   linearized suicide-vector pDS132, then transformed into *E. coli* DH5α. Conjugation and

425   selection of Δ*ulaG* and Δ*crp* mutants was performed in the same manner as described

426   for the Δ*vca0243* mutant. Primers used for construction of deletion mutants are listed in

427   Table S1. Restriction enzyme cut sites of SOE PCR primers are indicated by lowercase,

428   italicized letters. Complementary regions for Gibson assembly and SOE PCR are

429   represented by lowercase letters in each primer sequence. All primers utilized in this

430   study were purchased from IDT (Integrated DNA Technologies, Coralville, IA).

431   Deletion mutants were confirmed via PCR and DNA sequencing.

432   **_In vitro_ competition assays.** A *V. cholerae* Δ*lacZ* strain was utilized as a surrogate for

433   wild-type, as deletion of *lacZ* allows for subsequent blue/white colony selection when

434   plated on X-gal LB 1% plates. This mutant was shown to have no other defect compared

435   to wild type (23). *V. cholerae* Δ*lacZ* and genetic mutants were grown aerobically in LB 1%

436   for 24 hours, pelleted by centrifugation, washed and resuspended in PBS at a

437   concentration of 1×10^{10} CFU/mL. Cultures were then diluted in a 1:1 ratio

438   (mutant:Δ*lacZ*) and inoculated 1:50 into fully-filled and parafilmed 15mL conical tubes

439   containing M9CAS-Ascorbate or M9-CAS supplemented with 30 μg/mL mouse

440   intestinal mucus. Cultures were incubated anaerobically at 37°C in airtight containers

441   with GasPak EZ anaerobe sachets for 24 hours, then serially diluted and plated on X-gal

442   LB 1% plates. The competitive index (CI) of each strain was calculated using the

443   formula: CI = output ratio (Mutant / N16961Δ*lacZ*) / input ratio (Mutant / N16961Δ*lacZ*). The ratio of mutant

444   strain to Δ*lacZ* in the inoculum was referred to as the "input ratio", while the ratio of

445   mutant colonies to Δ*lacZ* colonies observed after competition was referred to as the

446   "output ratio". If an assay resulted in a CI > 1.0, the mutant outcompeted the wild-type;

447   while a CI < 1.0 indicated that the wild-type strain outcompeted the mutant.

448   **Bioinformatics analysis.** The YiaS and UlaG proteins of *E. coli* K-12 (NP_418613.2) were

449   used as seeds for BLASTp analysis against *V. cholerae* to identify putative L-ascorbate

450   catabolism proteins. The identified *V. cholerae* UlaG homolog VCA0248 (AWA79938.1)

451   was subsequently seeded for BLASTp analysis against other *Vibrionaceae* species.

452   Additionally, BLASTp analysis of the UlaA homolog VCA0246 (NP_232644.1) from *V.*

453   *cholerae* was performed against *Vibrionaceae* representative species in the NCBI genome

454   database. Analysis of VCA0243 (AAF96154.1, AWB75675.1) was also conducted using

455   BLASTp against *Vibrionaceae* and non-*Vibrio* species. Identified genomic regions were

456   downloaded from the National Center for Biotechnology Information (NCBI) database.

457   Figures representing amino acid similarity and gene cluster arrangement were

458   generated from genome sequences using tBLASTx in Easyfig 2.2.3 (42). Structural

459   analysis of VCA0243 by HHpred (43) was conducted using the protein FASTA sequence

460   (AAF96154.1) from NCBI.

461   **Growth phenotype assays.** Growth characteristics of *V. cholerae* N16961 and Δ*vca0243*

462   strains were examined on various carbon sources via a PM1 phenotype microarray

463   (Biolog, Inc., Hayward, CA). Briefly, aerobically grown LB 1% overnight cultures were

464   pelleted by centrifugation, washed with 1xPBS and resuspended in M9 minimal

465   containing 1% NaCl (M9). Cultures were then diluted 1:100 in M9, and 100μL was

466   inoculated into each well of a PM1 Biolog phenotype microarray. Cultures were

467   incubated at 37°C for 24 hours with intermittent shaking and the OD_{595nm} was measured

468   every hour utilizing a Tecan Sunrise microplate reader. Following assay completion, the

469   area under the curve (AUC) of each strain was calculated using Origin 2019 (OriginLab

470   Corporation, Northampton, MA). The AUC of the negative control (blank) was

471   subtracted from the AUC in each respective media, and the mean AUC of wild-type

472   and Δ*vca0243* were compared using an unpaired Student's *t*-test with 95% confidence

473   interval. A minimum of two biological replicates was performed for each strain.

474   **Phylogenetic analyses**. Phylogenetic analysis was conducted using UlaG (VCA0246)

475   and UlaD (VCA0240) protein as a seed to identity all homologs within the family

476   *Vibrionaceae* and their closest relatives. Unique protein sequences that had >95%

477   sequence coverage and >70% amino acid identity with UlaG and UalD were obtained

478   from NCBI database and aligned using the ClustalW (44). The housekeeping protein

479   RpoB was used to show the evolutionary relationships among all the species examined

480   in the UlaG and UlaD trees. The evolutionary history of each protein was inferred by

481   using the Maximum Likelihood method and Le_Gascuel_2008 model as determine by

482   best fit model selection in MEGAX (45, 46). The trees are drawn to scale, with branch

483   lengths measured in the number of substitutions per site. UlaG analysis involved 68,

484   UlaD 63 and RpoB 64 amino acid sequences. All positions with less than 95% site

485   coverage were eliminated, i.e., fewer than 5% alignment gaps, missing data, and

486   ambiguous bases were allowed at any position (partial deletion option). There were a

487   total of 354 positions for UlaG, 214 positions for UlaD, 1341 positions for RpoB in the

488   final dataset. Evolutionary analyses were conducted in MEGA (46).

489

490   ACKNOWLEDGEMENTS

494

495

496

497

498

499 **Table 1. Bacterial strain and plasmids used in this study**

Strain or Plasmid	Description	Source or Reference
Escherichia coli β2155λ*pir*	Transformation and plasmid isolation	Lab collection
Escherichia coli DH5αλ*pir*	Dap auxotroph; donor for bacterial conjugation	Lab collection
Escherichia coli BW25113	lacl^q, rrnB$_{T14}$, Δ*lacZ*$_{WJ16}$, *hsdR514*, Δ*rhaBAD*$_{LD78}$	Lab collection
Vibrio cholerae N16961	O1, El Tor Sm^r	(47)
Vibrio cholerae SAM2338	N16961 Δl*acZ*, *gfp*, Sm^r	(23)
Vibrio cholerae JPRA0248	N16961; in-frame deletion of L-ascorbate lactonase *vca0248* (*ulaG*)	This study
Vibrio cholerae JPRA0243	N16961; in-frame deletion of pyridoxal phosphatase *vca0243*	This study
Vibrio cholerae JPR2614	N16961; in-frame deletion of cAMP receptor protein *vc2614* (*crp*)	This study
Vibrio vulnificus CMCP6	Clinical Isolate	(48)
Vibrio parahaemolyticus RIMD2210633	Clinical Isolate	(49)
pDS132	Suicide vector; Cm^r, *sacB*	(50)
pDS132Δ*ulaG*	*VCA0248* knockout vector (VC_ulaG Gibson Product)	This study
pDS132Δ*vca0243*	*V. cholerae VCA0243* deletion vector (VCA0243 SOE Product)	This study
pDS132Δ*crp*	*VC2614* knockout vector (VC_crp Gibson Product)	This study

500

501

502   **Table 2. Primers**

Primer Name	Sequence (5' - 3')	Product size
SOE Primers		
VCA0243_A	*cacgagctc*GATGCCTAAATCGACCCATGC	506-bp
VCA0243_B	GCGATGGCCAATGCCGATGAC	
VCA0243_C	*gtcatcggcattggccatcgc*AAGCACATGACAATGCTGCTG	503-bp
VCA0243_D	*ggatctaga*GCTCAAGCGGGCATTGATATT	
VCA0243_FF	GTCCGGCAATAAAGGTTTTG	1911-bp
VCA0243_FR	CAAAGTGGTGGAAGGCAAAT	
Gibson Assembly Primers		
VC_ulaG_A	accgcatgcgatatcgagctGAAGATCACGATGATGTGATC	501-bp
VC_ulaG_B	aaaaggctttATTCACTTTACTCATAACAACACC	
VC_ulaG_C	taaagtgaatAAAGCCTTTTTGTAAGGATGAATG	501-bp
VC_ulaG_D	gtggaattcccgggagagctTCCTTTGGCGTGCTGATC	
VC_ulaG_Flank_FWD	GTGACCAACTATTTTCCGTTG	2145-bp
VC_ulaG_Flank_REV	ATCGGAGCCTATCTATCCGAC	
ulaG_A	GAAGATCACGATGTGATC	2040-bp
ulaG_D	TCCTTTGGCGTGCTGATC	
VC_CRP_A	accgcatgcgatatcgagctGTTCCTACGGTCGATACTTCT	504-bp
VC_CRP_B	tgccgtaaacACCTAGAACCATAATAATCTCAC	
VC_CRP_C	ggttctaggtGTTTACGGCACTCGCTAAGTG	501-bp

VC_CRP_D	gtggaattcccgggagagctGGCGGTCGCTTATGGAGC	
VC_CRP_FWD	ATTGGTATGGTGCCGATTGT	1850-bp
VC_CRP_REV	CTGCAAGCGATTGTTGAAAA	
CRP_A	GTTCCTACGGTCGATACTTCT	1608-bp
CRP_D	GGCGGTCGCTTATGGAGC	
qPCR Primers		
VCA0246QF	ATGATGCCGAAGAACACCGT	138-bp
VCA0246QR	GATCGCCACCAAAATCGCTC	
VCA0247QF	AAAGTGCGTAATGGGGCAGA	143-bp
VCA0247QR	ACCACACTATCGCCTGGTTG	
VCA0248QF	GATGAGCGAGCCGTCAACTA	139-bp
VCA0248QR	TCTCACCGTACGACAGCAAC	
VC1730QF	ACTTTCACATAGCCACGGTC	151-bp
VC1730QR	TCAGCCTAGATCCGAAACAG	

503

504 **Figure Legends**

505 **Fig. 1. Pathways of L-ascorbate catabolism genes and pathways. A.** Ula system gene

506 order in *E. coli* K-12 and *V. cholerae* N16961. Gray bars indicate amino acid similarity via

507 tBLASTx. **B**. In anaerobic catabolism the transport and phosphorylation of L-ascorbate

508 to L-ascorbate-6-phosphate occurs via *ulaABC*, which encodes a PTS-type transporter.

509 L-ascorbate-6P is first converted to 3-keto-L-gulonate-6-P by the lactonase UlaG.

510 Subsequent conversion to D-xylulose-5-P occurs via UlaDEF, which can be further

511 catabolized by the Pentose Phosphate Pathway (PPP). In aerobic catabolism L-ascorbate

512 is also transported into the cell via UlaABC. 2,3-diketogulonate is produced from L-

513 ascorbate in the presence of oxygen and YiaK and YiaP can convert this to 3-keto-L-

514 gulonate-6-P. YiaQRS are paralogs of UlaDEF.

515 **Fig. 2. Growth of *Vibrio* strains on L-ascorbate**. (A) *E. coli* BW25113, (B) *V. cholerae*

516 N16961, (C) *V. vulnificus* CMCP6 and (D) *V. parahaemolyticus* RIMD2210633 were grown

517 in either M9CAS (squares), M9CAS-Glucose (circles), or M9CAS-ascorbate (triangles).

518 Cells were grown statically under microaerophilic conditions for 48 hours. Error bars

519 indicate standard deviation of the mean of two biological replicates.

520 **Fig. 3. Growth of *V. cholerae* wild type and Δ*ulaG*.** Wild type and Δ*ulaG* (Δ*vca0248*)

521 were grown in M9CAS-Ascorbate statically under anaerobic conditions for 48 hours.

522 Error bars indicate standard deviation of the mean of two biological replicates.

523 **Fig. 4. Expression analysis of L-ascorbate utilization genes.** Expression analysis of

524 *ulaA* (*vca0246*), *ulaR* (*vca0247*), and *ulaG* (*vca0248*) were performed from cells grown

525 microaerophilically in (A) M9CAS-Ascorbate relative to M9CAS-Glucose (B) M9CAS-

526 Ascorbate relative to M9CAS and (C) M9-Mucus relative to cells M9CAS-Glucose. Data

527 represent the mean fold change of two independent biological replicates. Error bars

528 indicate standard deviation. Expression was normalized to the house keeping gene *topI.*

529 A Student's *t*-test was used to compare mean ΔC_T values between given conditions. *

530 p<0.05, ** p<0.01, *** p<0.001.

531 **Fig. 5. *In vitro* Competition assays**. *V. cholerae* Δ*lacZ* and Δ*ulaG* strains were grown in

532 1:1 ratio in M9-Ascorbate or M9CAS-Mucus overnight and cells counted from a

533 blue/white screen. Competitive Index (CI) was calculated using the formula: CI = output

534 ratio (Δ*ulaG*/ Δ*lacZ*) / input ratio (Δ*ulaG* / Δ*lacZ*).

535 **Fig. 6. Growth analysis of *V. cholerae* N16961and Δ*vca0243*.** Wild type or Δ*vca0243*

536 were grown in **A.** M9CAS-Ascorbate or **B.** M9-Ascorbate under anaerobic conditions for

537 48 hours at 37°C. Wild type and Δ*vca0243* were grown in **C.** M9CAS-Glucose or **D.** M9-

538 Glucose under aerobic conditions for 24 hours at 37°C. Error bars indicate standard

539 deviation of the mean of two biological replicates. End-point biomass comparisons

540 were performed using an unpaired Student's *t*-test with a 95% confidence interval.

541 *p<0.05 ***p<0.001

542 **Fig. 7. Growth analysis of *V. cholerae* N16961 and Δ*crp* on L-ascorbate**. Wild type and

543 Δ*crp* were grown in **A.** M9CAS-Glucose or **B.** M9CAS-Ascorbic acid. Cells were grown

544 statically under anaerobic conditions for 24 hours. Error bars indicate standard

545 deviation of the mean of two biological replicates.

546 **Fig. 8. Evolutionary analysis of UlaG.** The UlaG Maximum Likelihood tree with the

547 highest log likelihood (-5835.54) is shown. The percentage of trees in which the

548 associated taxa clustered together is shown next to the branches. Initial tree(s) for the

549 heuristic search were obtained automatically by applying Neighbor-Join and BioNJ

550 algorithms to a matrix of pairwise distances estimated using a JTT model, and then

551 selecting the topology with superior log likelihood value. A discrete Gamma

552 distribution was used to model evolutionary rate differences among sites (3 categories

553 (+*G*, parameter = 0.3678)).

554 **Supplemental Data**

555 **Fig. S1. A. Growth of *V. cholerae* wild type and Δ*ulaG*. A.** Growth in LB 1%NaCl. for

556 24 hours. Growth in B. M9CAS or C. M9CAS-Glucose anaerobically for 48 hours. Error

557 bars indicate standard deviation of the mean of two biological replicates.

558 **Fig. S2. Growth of *V. cholerae* wild type and Δ*vca0243*** in LB aerobically Cells were

559 grown 24 hours. Error bars indicate standard deviation of the mean of two biological

560 replicates.

561 **Fig. S3. Growth of *V. cholerae* N16961 and Δ*vca0243* on various carbon sources.** *V.*

562 *cholerae* N16961 (black bars) and Δ*vca0243* (white bars) were diluted in M9 minimal

563 media and grown aerobically for 24 hours on various carbon sources in a PM1 Biolog

564 Phenotype Microarray. Carbon utilization results of non-amino acid sources are

565 included in **A**-**C**. Use of amino acids and derivatives are displayed in **D**. Mean AUC

566 was calculated for each carbon source in Origin 2019. Error bars indicate standard error

567 of the mean of two biological replicates. Mean AUC comparison was performed

568 utilizing an unpaired Students *t*-test with 95% confidence interval. *p<0.05, **p<0.01,

569 ***p<0.001. (N-A-G: *N*-acetylglucosamine).

570 **Fig. S4. A. *Vibrionaceae* housekeeping tree based on RpoB using the Neighbor-**

571 **Joining method.** The optimal tree with the sum of branch length = 1.18 is shown. The

572 bootstrap test (500 replicates) values are shown next to the branches. The evolutionary

573 distances were computed using the JTT matrix-based method and are in the units of the

574 number of amino acid substitutions per site. The rate variation among sites was

575 modeled with a gamma distribution (shape parameter = 5). This analysis involved 64

576 amino acid sequences. There were a total of 1341 positions in the final dataset. Bacterial

577 families to which each species belongs are labelled and major clades of *Vibrio* species are

578 named in orange. **B.** The *ula* gene clusters present among the strains examined. Arrows

579 indicate ORFs and the direction of transcription and black lines indicate genes are

580 contiguous. Homologous genes are colored similarly.

581 **Fig. S5. Evolutionary analysis of UlaD among Vibrionaceae.** UlaD Neighbor-joining tree.

582 The optimal tree with the sum of branch length = 3.8 is shown. Bootstrap test (500 replicates)

583 values are shown next to the branches. The evolutionary distances were computed using the

584 JTT matrix-based method and are in the units of the number of amino acid substitutions per

585 site. The rate variation among sites was modeled with a gamma distribution (shape parameter =

586 5). This analysis involved 63 amino acid sequences. There were a total of 214 positions in the

587 final dataset.

588 **Fig. S6. Unique clustering of aerobic and anaerobic L-ascorbate catabolism operons**.

589 The Yia/Ula gene clusters group together on the genomes of species from the Spendidus clade.

590 Arrow depict ORFs and direction of arrows indicate direction of transcription. Purple arrows

591 labelled YbhA indicate the two copies of the pyroxidal phosphatase.

592

593

594

595 1. Traber M, Stevens J. 2011. Vitamins C and E: beneficial effects from a mechanistic perspective.
596   Free Radic Biol Med 51:1000-13. .
597 2. Granger M, Eck P. 2018. Dietary Vitamin C in Human Health. Adv Food Nutr Res 83:281-310.
598 3. Carr AC, Maggini S. 2017. Vitamin C and Immune Function. Nutrients 9.
599 4. Chatterjee IB, Kar NC, Ghosh NC, Guha BC. 1961. Aspects of ascorbic acid biosynthesis in
600   animals. Ann N Y Acad Sci 92:36-56.
601 5. Drouin G, Godin JR, Pagé B. 2011. The genetics of vitamin C loss in vertebrates. Curr Genomics
602   12:371-8.
603 6. Henriques SF, Duque P, Lopez-Fernandez H, Vazquez N, Fdez-Riverola F, Reboiro-Jato M, Vieira
604   CP, Vieira J. 2019. Multiple independent L-gulonolactone oxidase (GULO) gene losses and
605   vitamin C synthesis reacquisition events in non-Deuterostomian animal species. BMC Evol Biol
606   19:126.
607 7. Campos E, Aguilar J, Baldoma L, Badia J. 2002. The gene yjfQ encodes the repressor of the yjfR-X
608   regulon (ula), which is involved in L-ascorbate metabolism in Escherichia coli. J Bacteriol
609   184:6065-8.
610 8. Campos E, Aguilera L, Gimenez R, Aguilar J, Baldoma L, Badia J. 2009. Role of YiaX2 in L-
611   ascorbate transport in Klebsiella pneumoniae 13882. Can J Microbiol 55:1319-22.
612 9. Campos E, de la Riva L, Garces F, Gimenez R, Aguilar J, Baldoma L, Badia J. 2008. The
613   yiaKLX1X2PQRS and ulaABCDEFG gene systems are required for the aerobic utilization of L-
614   ascorbate in Klebsiella pneumoniae strain 13882 with L-ascorbate-6-phosphate as the inducer. J
615   Bacteriol 190:6615-24.
616 10. Campos E, Montella C, Garces F, Baldoma L, Aguilar J, Badia J. 2007. Aerobic L-ascorbate
617   metabolism and associated oxidative stress in Escherichia coli. Microbiology (Reading) 153:3399-
618   3408.
619 11. Yew WS, Gerlt JA. 2002. Utilization of L-ascorbate by Escherichia coli K-12: assignments of
620   functions to products of the yjf-sga and yia-sgb operons. J Bacteriol 184:302-6.
621 12. Zhang Z, Aboulwafa M, Smith MH, Saier MH, Jr. 2003. The ascorbate transporter of Escherichia
622   coli. J Bacteriol 185:2243-50.
623 13. Campos E, Baldoma L, Aguilar J, Badia J. 2004. Regulation of expression of the divergent ulaG
624   and ulaABCDEF operons involved in LaAscorbate dissimilation in Escherichia coli. J Bacteriol
625   186:1720-8.
626 14. Colwell RR, Huq A, Chowdhury MA, Brayton PR, Xu B. 1995. Serogroup conversion of *Vibrio*
627   *cholerae*. Can J Microbiol 41:946-50.
628 15. Faruque SM, Albert MJ, Mekalanos JJ. 1998. Epidemiology, genetics, and ecology of toxigenic
629   Vibrio cholerae. Microbiol Mol Biol Rev 62:1301-14.
630 16. Thelin K, Taylor R. 1996. Toxin-coregulated pilus, but not mannose-sensitive hemagglutinin, is
631   required for colonization by *Vibrio cholerae* O1 El Tor biotype and O139 strains. Infect Immun
632   64:2853-2856. .
633 17. Waldor MK, Mekalanos JJ. 1996. Lysogenic conversion by a filamentous phage encoding cholera
634   toxin. Science 272:1910-4.
635 18. Liu M, Hao G, Li Z, Zhou Y, Garcia-Sillas R, Li J, Wang H, Kan B, Zhu J. 2019. CitAB Two-
636   Component System-Regulated Citrate Utilization Contributes to Vibrio cholerae Competitiveness
637   with the Gut Microbiota. Infect Immun 87.
638 19. Wang J, Xing X, Yang X, Jung IJ, Hao G, Chen Y, Liu M, Wang H, Zhu J. 2018. Gluconeogenic
639   growth of Vibrio cholerae is important for competing with host gut microbiota. J Med Microbiol
640   67:1628-1637.
641 20. Midani FS, Weil AA, Chowdhury F, Begum YA, Khan AI, Debela MD, Durand HK, Reese AT,
642   Nimmagadda SN, Silverman JD, Ellis CN, Ryan ET, Calderwood SB, Harris JB, Qadri F, David LA,

643   LaRocque RC. 2018. Human Gut Microbiota Predicts Susceptibility to Vibrio cholerae Infection. J
644   Infect Dis 218:645-653.
645   21.   Logan SL, Thomas J, Yan J, Baker RP, Shields DS, Xavier JB, Hammer BK, Parthasarathy R. 2018.
646   The Vibrio cholerae type VI secretion system can modulate host intestinal mechanics to displace
647   gut bacterial symbionts. Proc Natl Acad Sci U S A 115:E3779-E3787.
648   22.   Zhao W, Caro F, Robins W, Mekalanos JJ. 2018. Antagonism toward the intestinal microbiota and
649   its effect on Vibrio cholerae virulence. Science 359:210-213.
650   23.   Almagro-Moreno S, Boyd EF. 2009. Sialic acid catabolism confers a competitive advantage to
651   pathogenic vibrio cholerae in the mouse intestine. Infect Immun 77:3807-16.
652   24.   Almagro-Moreno S, Boyd EF. 2009. Insights into the evolution of sialic acid catabolism among
653   bacteria. BMC Evol Biol 9:118.
654   25.   McDonald ND, Lubin JB, Chowdhury N, Boyd EF. 2016. Host-Derived Sialic Acids Are an
655   Important Nutrient Source Required for Optimal Bacterial Fitness In Vivo. mBio 7:e02237-15.
656   26.   Reddi G, Pruss K, Cottingham KL, Taylor RK, Almagro-Moreno S. 2018. Catabolism of mucus
657   components influences motility of Vibrio cholerae in the presence of environmental reservoirs.
658   PLoS One 13:e0201383.
659   27.   Kalburge SS, Carpenter MR, Rozovsky S, Boyd EF. 2017. Quorum Sensing Regulators Are
660   Required for Metabolic Fitness in Vibrio parahaemolyticus. Infect Immun 85.
661   28.   Whitaker WB, Richards GP, Boyd EF. 2014. Loss of sigma factor RpoN increases intestinal
662   colonization of Vibrio parahaemolyticus in an adult mouse model. Infect Immun 82:544-56.
663   29.   Sugimoto R, Saito N, Shimada T, Tanaka K. 2018. Identification of YbhA as the pyridoxal 5'-
664   phosphate (PLP) phosphatase in Escherichia coli: Importance of PLP homeostasis on the
665   bacterial growth. J Gen Appl Microbiol 63:362-368.
666   30.   Savery N, Rhodius V, Busby S. 1996. Protein-protein interactions during transcription activation:
667   the case of the Escherichia coli cyclic AMP receptor protein. Philos Trans R Soc Lond B Biol Sci
668   351:543-50.
669   31.   Colton DM, Stabb EV. 2016. Rethinking the roles of CRP, cAMP, and sugar-mediated global
670   regulation in the Vibrionaceae. Curr Genet 62:39-45.
671   32.   Green J, Stapleton MR, Smith LJ, Artymiuk PJ, Kahramanoglou C, Hunt DM, Buxton RS. 2014.
672   Cyclic-AMP and bacterial cyclic-AMP receptor proteins revisited: adaptation for different
673   ecological niches. Curr Opin Microbiol 18:1-7.
674   33.   Boyd EF, Carpenter MR, Chowdhury N, Cohen AL, Haines-Menges BL, Kalburge SS, Kingston JJ,
675   Lubin JB, Ongagna-Yhombi SY, Whitaker WB. 2015. Post-Genomic Analysis of Members of the
676   Family Vibrionaceae. Microbiol Spectr 3.
677   34.   Kwong WK, Moran NA. 2013. Cultivation and characterization of the gut symbionts of honey
678   bees and bumble bees: description of Snodgrassella alvi gen. nov., sp. nov., a member of the
679   family Neisseriaceae of the Betaproteobacteria, and Gilliamella apicola gen. nov., sp. nov., a
680   member of Orbaceae fam. nov., Orbales ord. nov., a sister taxon to the order 'Enterobacteriales'
681   of the Gammaproteobacteria. Int J Syst Evol Microbiol 63:2008-2018.
682   35.   Pieper R, Zhang Q, Clark DJ, Parmar PP, Alami H, Suh MJ, Kuntumalla S, Braisted JC, Huang ST,
683   Tzipori S. 2013. Proteomic View of Interactions of Shiga Toxin-Producing Escherichia coli with
684   the Intestinal Environment in Gnotobiotic Piglets. PLoS One 8:e66462.
685   36.   Griesenauer B, Tran TM, Fortney KR, Janowicz DM, Johnson P, Gao H, Barnes S, Wilson LS, Liu Y,
686   Spinola SM. 2019. Determination of an Interaction Network between an Extracellular Bacterial
687   Pathogen and the Human Host. mBio 10.
688   37.   Richts B, Rosenberg J, Commichau FM. 2019. A Survey of Pyridoxal 5'-Phosphate-Dependent
689   Proteins in the Gram-Positive Model Bacterium Bacillus subtilis. Front Mol Biosci 6:32.

690 38. Percudani R, Peracchi A. 2003. A genomic overview of pyridoxal-phosphate-dependent enzymes.
691   EMBO Rep 4:850-4.
692 39. Schneider G, Käck H, Lindqvist Y. 2000. The manifold of vitamin B6 dependent enzymes.
693   Structure 8:R1-6.
694 40. Pfaffl MW. 2001. A new mathematical model for relative quantification in real-time RT-PCR. .
695   Nucleic Acids Res 29:e45.
696 41. Horton RM, Hunt HD, Ho SN, Pullen JK, Pease LR. 1989. Engineering hybrid genes without the
697   use of restriction enzymes: gene splicing by overlap extension. Gene 77:61-8.
698 42. Sullivan MJ, Petty NK, Beatson SA. 2011. Easyfig: a genome comparison visualizer. Bioinformatics
699   27:1009-10.
700 43. Zimmermann L, Stephens A, Nam SZ, Rau D, Kübler J, Lozajic M, Gabler F, Söding J, Lupas AN,
701   Alva V. 2018. A Completely Reimplemented MPI Bioinformatics Toolkit with a New HHpred
702   Server at its Core. J Mol Biol 430:2237-2243.
703 44. Larkin MA, Blackshields G, Brown NP, Chenna R, McGettigan PA, McWilliam H, Valentin F,
704   Wallace IM, Wilm A, Lopez R, Thompson JD, Gibson TJ, Higgins DG. 2007. Clustal W and Clustal X
705   version 2.0. Bioinformatics 23:2947-8.
706 45. Le SQ, Gascuel O. 2008. An improved general amino acid replacement matrix. Mol Biol Evol
707   25:1307-20.
708 46. Kumar S, Stecher G, Li M, Knyaz C, Tamura K. 2018. MEGA X: Molecular Evolutionary Genetics
709   Analysis across Computing Platforms. Mol Biol Evol 35:1547-1549.
710 47. Heidelberg JF, Eisen JA, Nelson WC, Clayton RA, Gwinn ML, Dodson RJ, Haft DH, Hickey EK,
711   Peterson JD, Umayam L, Gill SR, Nelson KE, Read TD, Tettelin H, Richardson D, Ermolaeva MD,
712   Vamathevan J, Bass S, Qin H, Dragoi I, Sellers P, McDonald L, Utterback T, Fleishmann RD,
713   Nierman WC, White O, Salzberg SL, Smith HO, Colwell RR, Mekalanos JJ, Venter JC, Fraser CM.
714   2000. DNA sequence of both chromosomes of the cholera pathogen Vibrio cholerae. Nature
715   406:477-83.
716 48. Chen CY, Wu KM, Chang YC, Chang CH, Tsai HC, Liao TL, Liu YM, Chen HJ, Shen AB, Li JC, Su TL,
717   Shao CP, Lee CT, Hor LI, Tsai SF. 2003. Comparative genome analysis of Vibrio vulnificus, a
718   marine pathogen. Genome Res 13:2577-87.
719 49. Makino K, Oshima K, Kurokawa K, Yokoyama K, Uda T, Tagomori K, Iijima Y, Najima M, Nakano
720   M, Yamashita A, Kubota Y, Kimura S, Yasunaga T, Honda T, Shinagawa H, Hattori M, Iida T. 2003.
721   Genome sequence of Vibrio parahaemolyticus: a pathogenic mechanism distinct from that of V
722   cholerae. Lancet 361:743-9.
723 50. Philippe N, Alcaraz JP, Coursange E, Geiselmann J, Schneider D. 2004. Improvement of pCVD442,
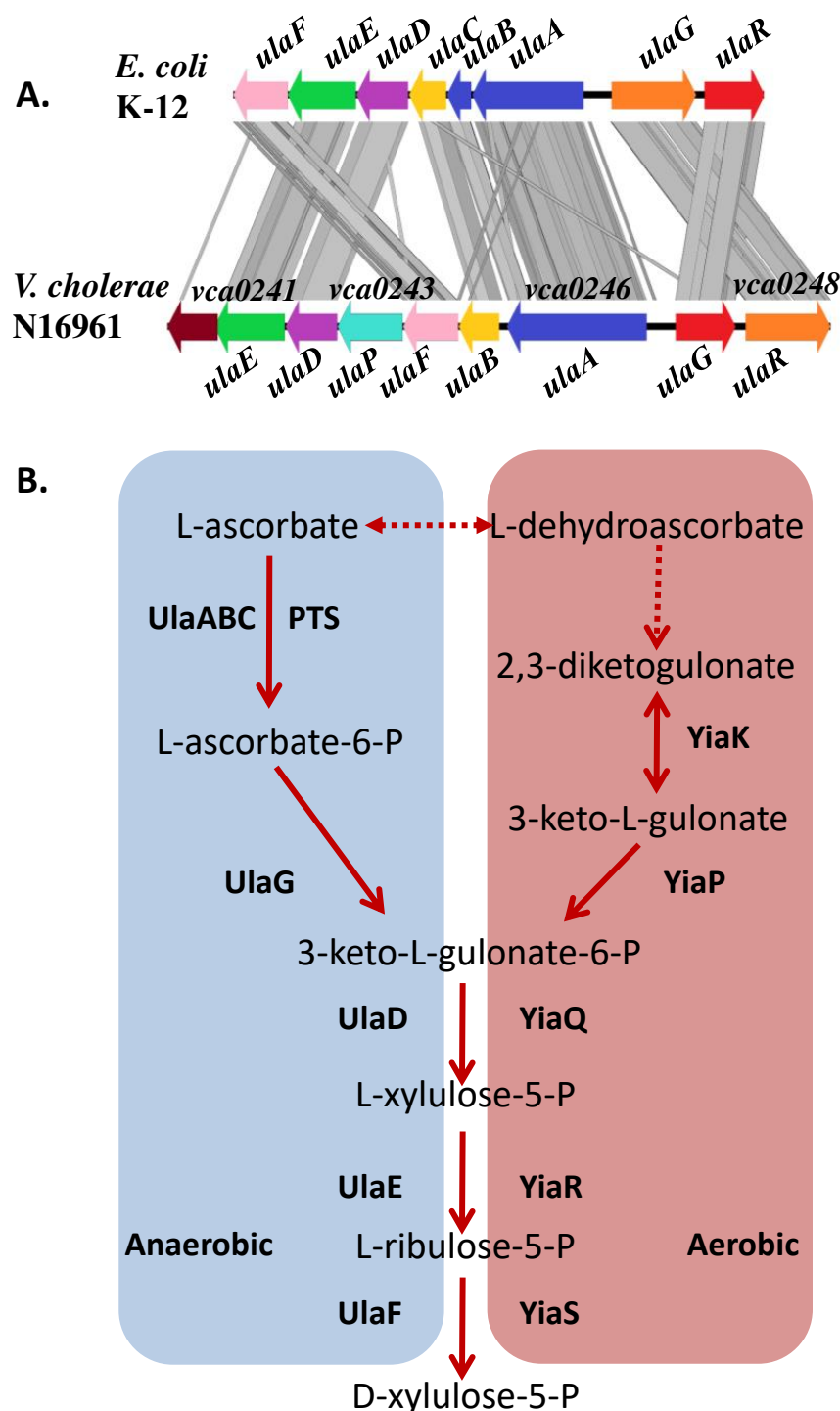724   a suicide plasmid for gene allele exchange in bacteria. Plasmid 51:246-55.
725

Fig. 1. Pathways of L-ascorbate catabolism genes and pathways. **A**. Ula system gene order in *E. coli* K-12 and *V. cholerae* N16961. Gray bars indicate amino acid similarity via tBLASTx **B**. In anaerobic catabolism the transport and phosphorylation of L-ascorbate to L-ascorbate-6-phosphate occurs via *ulaABC*, which encodes a PTS-type transporter. L-ascorbate-6P is first converted to 3-keto-L-gulonate-6-P by the lactonase UlaG. Subsequent conversion to D-xylulose-5-P occurs via UlaDEF, which can be further catabolized by the Pentose Phosphate Pathway (PPP). In aerobic catabolism L-ascorbate is also transported into the cell via UlaABC. 2,3-diketogulonate is produced from L-ascorbate in the presence of oxygen and YiaK and YiaP can convert this to 3-keto-L-gulonate-6-P. YiaQRS are paralogs of UlaDEF.
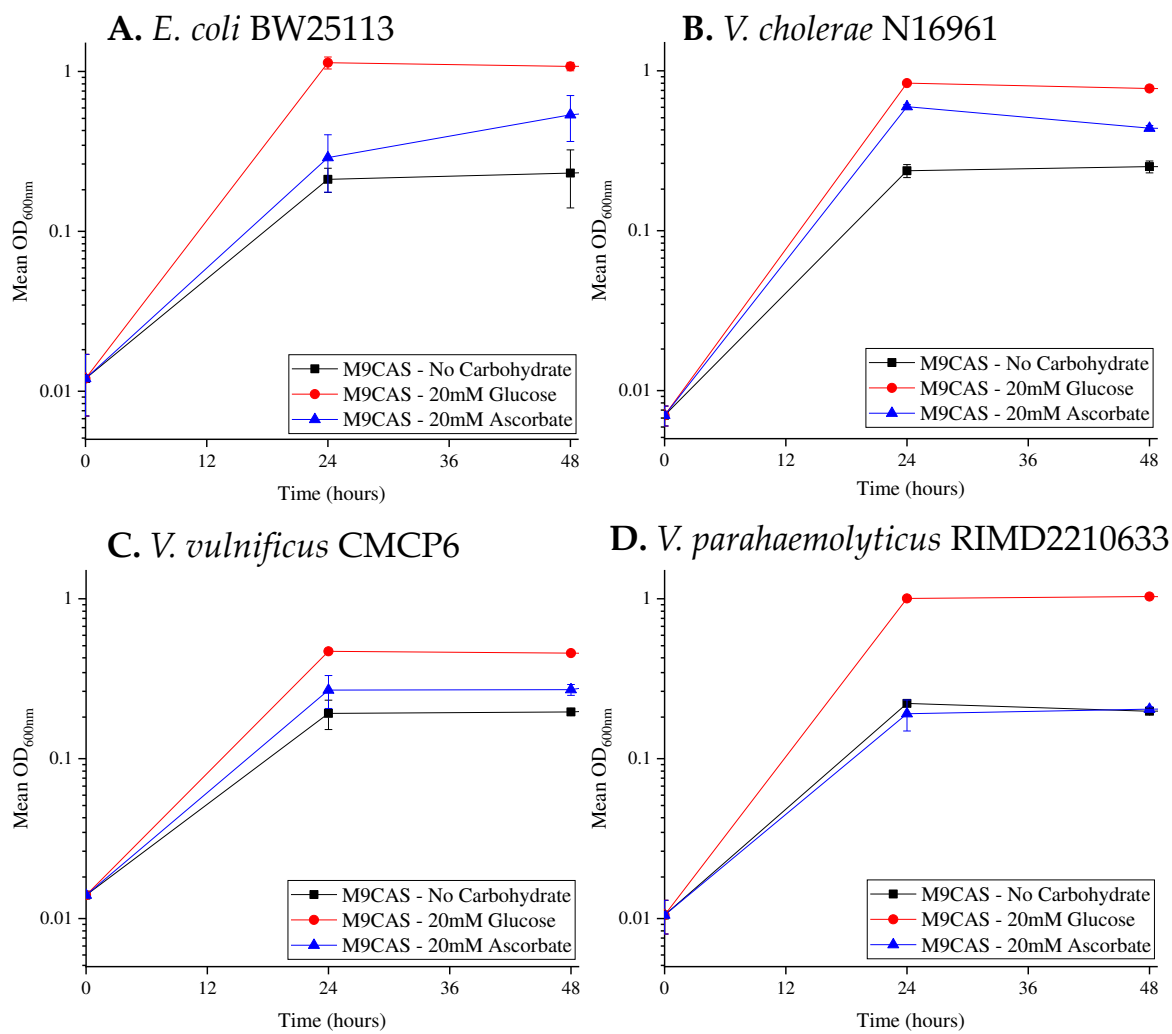
Fig. 2. Growth analysis of *Vibrio* strains on L-ascorbate. (**A**) *E. coli* BW25113, (**B**) *V. cholerae* N16961, (**C**) *V. vulnificus* CMCP6 and (**D**) *V. parahaemolyticus* RIMD2210633 were grown in either M9CAS (squares), M9CAS-Glucose (circles), or M9CAS-ascorbate (triangles). Cells were grown statically under microaerophilic conditions for 48 hours. Error bars indicate standard deviation of the mean of two biological replicates.
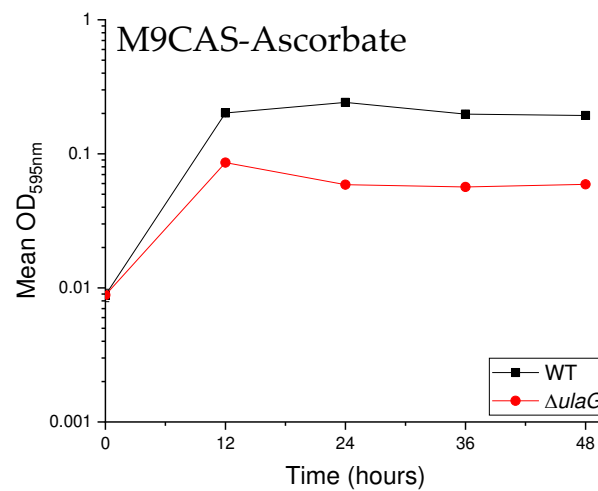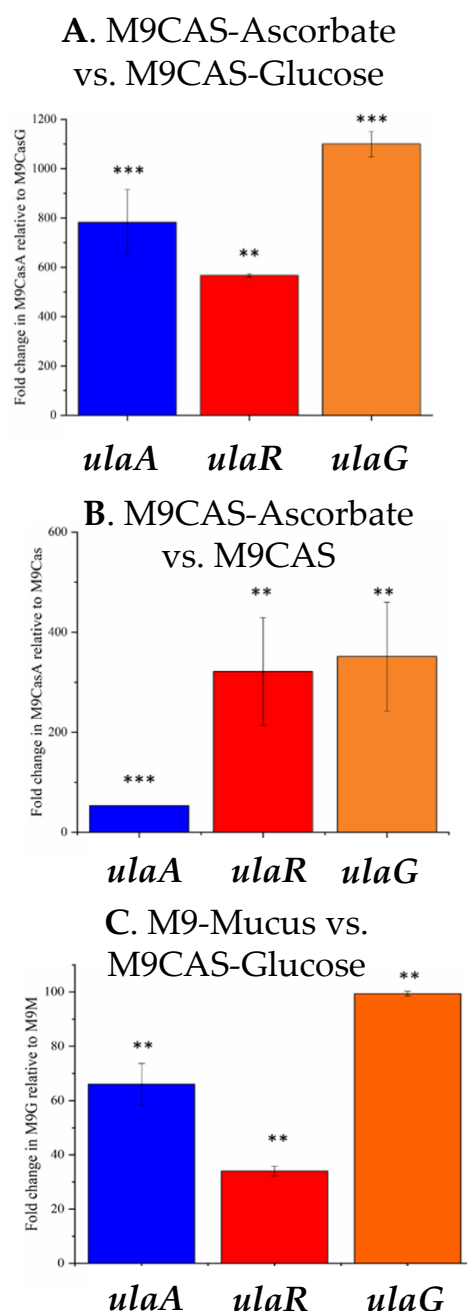
Fig. 3. Growth analysis of *V. cholerae* N16961 and Δ*ulaG*. Wild type and Δ*ulaG* (Δ*vca0248*) were grown in M9CAS-Ascorbate statically under anaerobic conditions for 48 hours. Error bars indicate standard deviation of the mean of two biological replicates.

Fig. 4. Expression analysis of L-ascorbate utilization genes. Expression analysis of *ulaA* (*vca0246*), *ulaR* (*vca0247*), and *ulaG* (*vca0248*) were performed from cells grown microaerophilically in **A.** M9CAS-Ascorbate relative to M9CAS-Glucose **B.** M9CAS-Ascorbate relative to M9CAS and **C.** M9-Mucus relative to cells M9CAS-Glucose. Data represent the mean fold change of two independent biological replicates. Error bars indicate standard deviation. Expression was normalized to the house keeping gene *topI*. A Student's *t*-test was used to compare mean ΔC_T values between given conditions. * $p<0.05$, ** $p<0.01$, *** $p<0.001$.
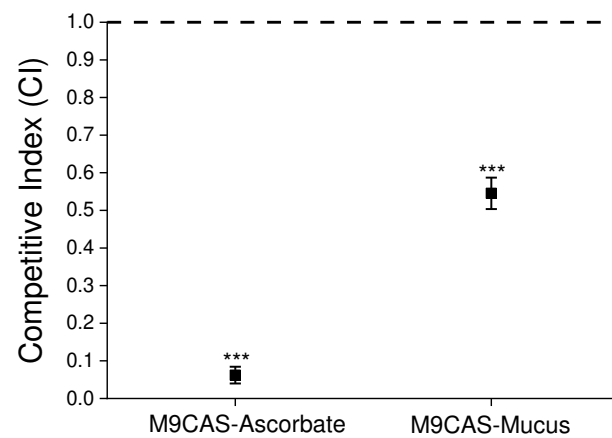
Fig. 5. *In vitro* Competition assays. *V. cholerae ΔlacZ* and *ΔulaG* strains were grown in 1:1 ratio in M9-Ascorbate or M9CAS-Mucus overnight and cells counted from a blue/white screen. Competitive Index (CI) was calculated using the formula: CI = output ratio $_{(\Delta ulaG/ \Delta lacZ)}$ / input ratio $_{(\Delta ulaG / \Delta lacZ)}$.
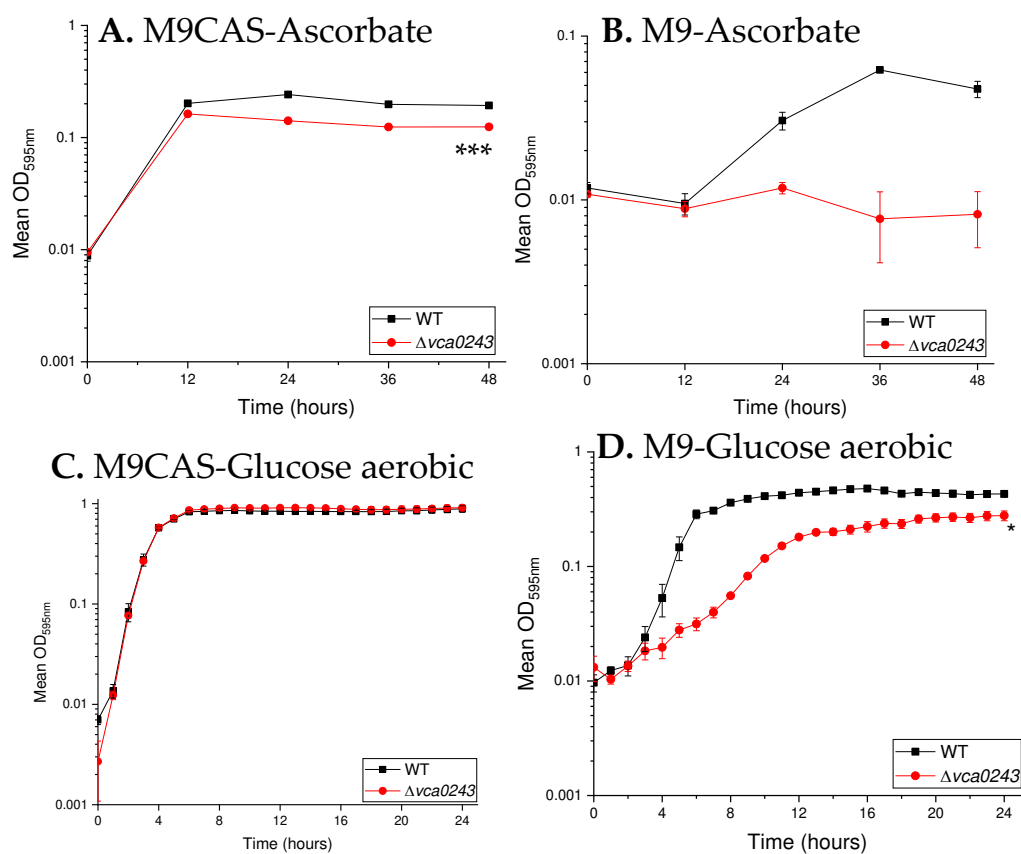
Fig. 6. Growth analysis of *V. cholerae* N16961and Δ*vca0243*. Wild type and Δ*vca0243* were grown in **A**. M9CAS-Ascorbate or **B**. M9-Ascorbate under anaerobic conditions for 48 hours at 37ºC. Wild type and Δ*vca0243* were grown in **C**. M9CAS-Glucose or **D**. M9-Glucose under aerobic conditions for 24 hours at 37ºC. Error bars indicate standard deviation of the mean of two biological replicates. End-point biomass comparisons were performed using an unpaired Student's *t*-test with a 95% confidence interval. *p<0.05 ***p<0.001
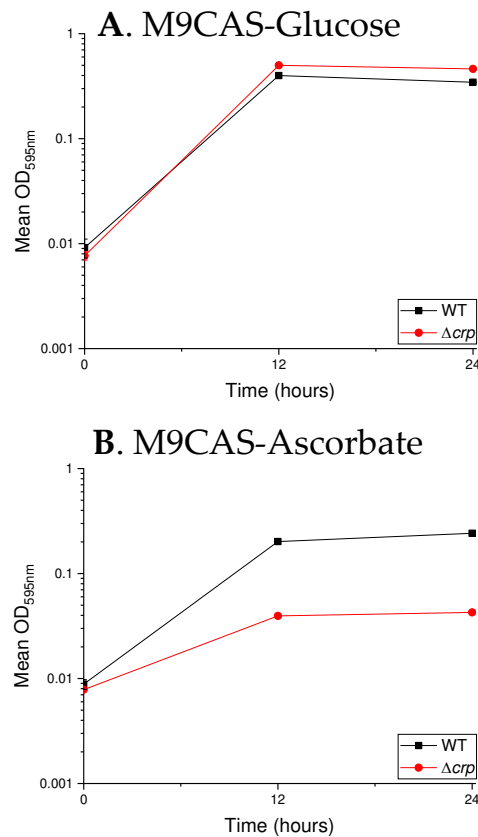
Fig. 7. Growth analysis of *V. cholerae* N16961 and Δ*crp* on L-ascorbate. Wild type and Δ*crp* were grown in either **A**. M9CAS-Glucose or **B**. M9CAS-Ascorbic acid Cells were grown statically under anaerobic conditions for 24 hours. Error bars indicate standard deviation of the mean of two biological replicates.